

## POTENTIALITIES OF MODIFICATION OF METAL OXIDE VARISTOR MICROSTRUCTURES\*

Witold Mielcarek<sup>1</sup>, Krystyna Prociów<sup>1</sup>, Joanna Warycha<sup>1</sup>

The electrical properties of varistors, similarly like posistors and other devices made of semiconducting ceramic, are controlled by grain boundaries. In varistor conductivity the main role play potential barriers which arise at grain boundaries during varistor sintering. The I-V behavior of varistor ceramic is such that during conduction the varistor voltage remains relatively constant while a current changes are of several orders of magnitude.

Varistor is produced by sintering a mixture of ZnO with a small addition of Bi<sub>2</sub>O<sub>3</sub> and other metal oxides. Varistor microstructure composes of ZnO grains. Each ZnO grain acts as it has a semiconducting junction at the grain boundary. The non-linear electrical behavior occurs at the boundary of each ZnO grain. The junctions between grains are separated by an intergranular phase. The best varistor performance is attained when the Bi-rich intergranular layer is of nanometer size. When the intergranular phase is in a shape of agglomerates embedding Bi<sub>2</sub>O<sub>3</sub> crystal phases and spinel grains it forms areas excluded from conduction. The problem has been studied with emphasis on determining the relation between ZnO dopants and microstructure evolution. It was established that the vulnerability of varistor ceramic for formation of agglomerates depend on the composition of additive oxides. With SrO, MnO and PbO varistor ceramic is more susceptible for formation of agglomerates, while Co<sub>2</sub>O<sub>3</sub>, Sb<sub>2</sub>O<sub>3</sub> and SnO<sub>2</sub> facilitates the homogenous distribution of additives in varistor body. Elimination of an electrically inactive areas from varistor body would enable the decrease of the amount of additives (e.g. the amount of Bi<sub>2</sub>O<sub>3</sub> would decrease from 1 mol % to 0.2 mol %) and bring about the diminishment of the cost of varistor processing along with improvement of varistor performance.

**Keywords:** ZnO varistor, microstructure, semiconducting ceramic, doping, Bi<sub>2</sub>O<sub>3</sub>

<sup>1)</sup> Electrotechnical Institute, ul. M. Skłodowskiej-Curie 55/61, 50-369 Wrocław, Poland

\* Praca prezentowana na XXXII International Conference of IMAPS - CPMP IEEE, Poland, Pułtusk, 21-24.09.2008

## 1. INTRODUCTION

Unwanted over-voltage-induced effects have accompanied electricity from the beginning of its discovery. Nowadays the negative impacts of these effects are successfully eliminated by using various protection devices, among others varistors, i.e., variable resistors (VRs).

Varistors have the ability to protect devices thanks to their non-linear current-voltage (I-V) characteristics. The first varistors were made of silicon carbide, but the non-linear coefficients of their I-V characteristics were rather low ( $\alpha = 6-8$ ).

The first paper on the non-linear properties of the ZnO-Bi<sub>2</sub>O<sub>3</sub> system was published by Kosman and Gesse [1], but Matsuoka [2] developed the ZnO-Bi<sub>2</sub>O<sub>3</sub> system and made it commercially useful; and for ZnO sintered with a small amount of other metal (Bi, Sb, Co, Mn, Ni) oxides he got  $\alpha$  coefficients in the range of a few tens.

A typical ZnO-varistor microstructure observed in the scanning electron microscope (SEM) is shown in Fig.1. The base ingredient of the varistor microstructure constitute ZnO grains separated by a Bi-rich phase and products of reactions of other metal-oxide additives between each other and with ZnO. The bright areas seen in Fig.1 are the Bi-rich inter-granular phase. The clusters of fine grains in it are particles of zinc-antimony spinel.

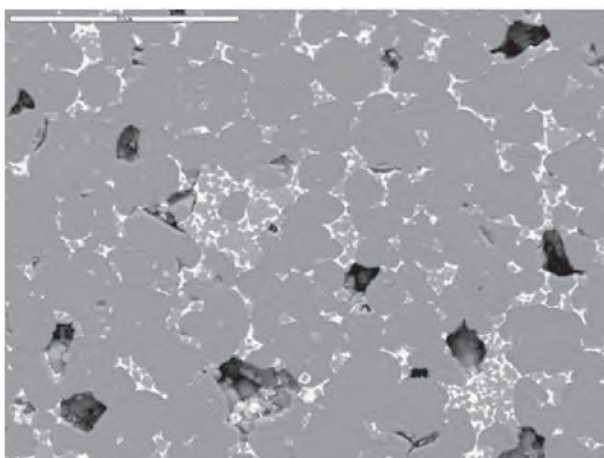


**Fig.1.** SEM image of the polished surface of ZnO varistor.

**Rys. 1.** Zdjęcie SEM struktury typowego warystora ZnO.

The paths of current flow in a varistor are shown in Fig. 2.

When a bulk of the varistor between contacts comprises of ZnO grains of different size, a voltage gradient measured across the varistor thickness is the result of voltage equalizing at the expense of a differentiation in the magnitude of the currents. In

result through the paths with the lowest number of grain boundaries flow the highest currents and areas with a large number of small grains are excluded from charge conduction, what means that they are useless elements of the varistor microstructure, contributing little or not at all to the protection characteristics.

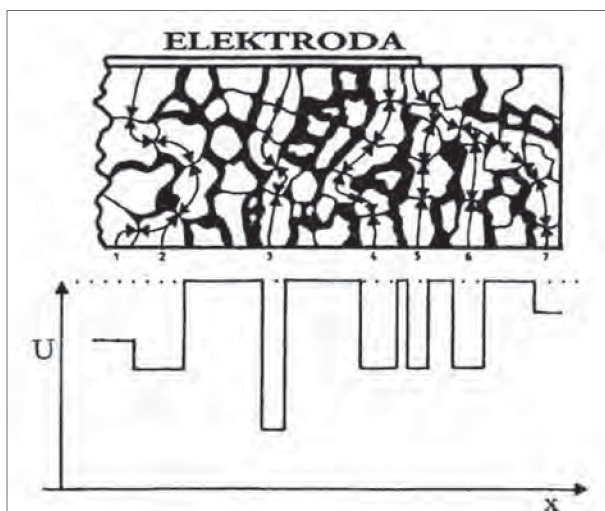


**Fig. 2.** Paths of current flow in a varistor [3].

**Rys. 2.** Ścieżki przepływu prądu w warystorze.

For good electrical performance the varistor requires a large number of boundaries with the proper profile of defects at the grain interface so as to sustain a voltage of  $\approx 3$  V per grain. It is attainable by wetting the grain interface with liquid  $\text{Bi}_2\text{O}_3$ . The  $\text{Bi}_2\text{O}_3$ 's ability to penetrate a ZnO grain and modify the barrier's shape is the best when the  $\text{Bi}_2\text{O}_3$  is in an amorphous form.

$\text{Bi}_2\text{O}_3$  occurs in numerous crystalline forms and readily reacts with other metal oxides and as a result forms over 500 compounds. The basic  $\text{Bi}_2\text{O}_3$  crystalline phases can also dissolve other elements, without changing their structures. The wettability of  $\text{Bi}_2\text{O}_3$  depends strongly on its crystalline form. The best wettability of ZnO grains has  $\alpha\text{-Bi}_2\text{O}_3$  form. The  $\delta\text{-Bi}_2\text{O}_3$  form does not have the ability to wet the ZnO grain boundaries. Potentialities of modification of varistor microstructure by modification of the  $\text{Bi}_2\text{O}_3$  with other metal oxide prior to adding it varistor powder mixture.

The selected  $\text{Bi}_2\text{O}_3$  modifiers were the metal oxides usually applied as ZnO varistor dopants and those with glaze-forming ability like Co, Mn, Sb, Si and Sn.

## 2. EXPERIMENT

$\text{Bi}_2\text{O}_3$  modifications of the  $(\text{Bi}_{0.85}\text{Me}_{0.15})_2\text{O}_3$  type were made and tested for crystal-phase composition. Next, the action of the modified  $\text{Bi}_2\text{O}_3$  forms was checked for the crystal-phase composition and microstructure development. Finally, from the same point of view, i.e., the crystal-phase composition and microstructure development, the modified forms of  $\text{Bi}_2\text{O}_3$  were verified in varistor compositions.

### 2.1. Preparation of the samples

To make the  $(\text{Bi}_{0.85}\text{Me}_{0.15})_2\text{O}_3$  samples, the mixtures of 85 mol%  $\text{Bi}_2\text{O}_3$  and 15 mol% of other metal oxide were mixed and milled in water for 18 hours and dried. After adding 7 wt % of binder, the mixtures were sieved using a nylon mesh, pressed in the form of discs, sintered at 770°C for 1 hour, cooled and grinded.

The composition of the varistor samples was as proposed by Matsuoka [2], with exception of  $\text{Bi}_2\text{O}_3$  that was in modified form. The details are given in Tab. 1.

**Table 1.** Composition of varistor samples.

**Tabela 1.** Skład ilościowy i jakościowy próbek.

Component	Quantity [mol %]
ZnO	95.8
$\text{Bi}_2\text{O}_3$	1.0
$\text{Sb}_2\text{O}_3$	1.0
$\text{Co}_2\text{O}_3$	0.5
MnO	0.5
$\text{Cr}_2\text{O}_3$	0.5
NiO	0.8

The varistor samples were sintered at 1250°C for 1 hour.

### 2.2. Methods of sample examination

The crystal phases were identified with DRON-2 diffractometer using Fe filtered Co  $K\alpha$  radiation. The XRD patterns were recorded in scan mode with  $\Delta 2\theta = 0.05^\circ$ . The crystal phases were identified by comparing the measured spectra with data of powder-diffraction files (PDF).

Images of the microstructures of varistor samples were taken with scanning electron microscope (SEM) Jeol JXA-5A X-ray microanalyser.



### 3. RESULTS

#### 3.1. Crystal phases identified in the $(\text{Bi}_{0.85}\text{Me}_{0.15})_2\text{O}_3$ systems

Crystal phases identified in the  $(\text{Bi}_{0.85}\text{Me}_{0.15})_2\text{O}_3$  systems are shown in Tab. 2. With  $\text{Co}_2\text{O}_3$  modifier the  $\text{Bi}_{25}\text{CoO}_{40}$  (PDF 39-871) phase, belonging to the  $\gamma$ -sillenite family. The  $(\text{Bi}_{0.85}\text{Mn}_{0.15})_2\text{O}_3$  sample with the MnO modifier was composed of  $\alpha$ - $\text{Bi}_2\text{O}_3$  (PDF27-53) and a traces of  $\text{Bi}_2\text{Mn}_4\text{O}_{10}$  (PDF27-48).

**Table 2.** Crystal phases identified in the  $(\text{Bi}_{0.85}\text{Me}_{0.15})_2\text{O}_3$  systems.

**Tabela 2.** Fazy krystaliczne zidentyfikowane w układach  $(\text{Bi}_{0.85}\text{Me}_{0.15})_2\text{O}_3$ .

Co	Mn	Pb	Sb	Al	Si	Sn
$\text{Bi}_{25}\text{CoO}_{40}$	$\text{Bi}_2\text{Mn}_4\text{O}_{10}$	$\text{Bi}_{24}\text{Pb}_2\text{O}_{40}$	$\beta\text{Bi}_2\text{O}_3$	$\text{A}_2\text{Bi}_{24}\text{O}_{39}$	$\text{Bi}_{12}\text{SiO}_{20}$	$\alpha\text{Bi}_2\text{O}_3$

In the  $(\text{Bi}_{0.85}\text{Pb}_{0.15})_2\text{O}_3$  sample,  $\text{Bi}_{24}\text{Pb}_2\text{O}_{40}$  (PDF22-1059), similar in structure to  $\text{Bi}_{12}\text{SiO}_{20}$  sillenite, and  $\text{Pb}_5\text{Bi}_8\text{O}_{17}$  (PDF38-125) were identified. The  $(\text{Bi}_{0.85}\text{Sb}_{0.15})_2\text{O}_3$  sample was composed mainly of  $\beta$ - $\text{Bi}_2\text{O}_3$  (PDF27-50) and traces of  $\delta$ - $\text{Bi}_2\text{O}_3$  (PDF27-52).

In the sample modified with  $\text{Al}_2\text{O}_3$ ,  $\text{Al}_2\text{Bi}_{24}\text{O}_{39}$  (PDF23-1005) phase, similar in structure to sillenite ( $\text{Bi}_{12}\text{SiO}_{20}$ ), and traces of corundum (PDF10-173) were identified. The  $(\text{Bi}_{0.85}\text{Si}_{0.15})_2\text{O}_3$  sample was composed of sillenite:  $\text{Bi}_{12}\text{SiO}_{20}$  (PDF37-485). The  $(\text{Bi}_{0.85}\text{Sn}_{0.15})_2\text{O}_3$  sample, with  $\text{Bi}_2\text{O}_3$  modified by Sn, was composed of  $\alpha$ - $\text{Bi}_2\text{O}_3$  (PDF27-53).

Concluding, the  $\text{Bi}_2\text{O}_3$  modification with the use of a metal additive at the rate of one metal atom to six atoms of bismuth brings about phases with a structure similar to sillenite ( $\text{Bi}_{12}\text{SiO}_{20}$ ), which is advantageous in varistor applications because of the low oxygen-ion conductivity of those phases.

#### 3.2. Microstructure and crystal phases identified in varistors doped with modified $\text{Bi}_2\text{O}_3$

As can be seen in Fig.2 varistor doped with unmodified  $\text{Bi}_2\text{O}_3$  has characteristic 20  $\mu\text{m}$  ZnO grains and a heterogeneous intergranular layer that forms clusters (bright zones in Fig. 3) 20 with large number of fine grains of zinc-antimony spinel (PDF15-687) inside them.

The other crystal phase present in the intergranular layer of the varistor with unmodified  $\text{Bi}_2\text{O}_3$  is  $\beta$ - $\text{Bi}_2\text{O}_3$  (PDF27-50). The  $\text{Co}_2\text{O}_3$  modifier (Fig. 3) had a positive effect on the intergranular phase distribution, but contributed to an increase in the quantity of the undesirable secondary phases in the varistor body.

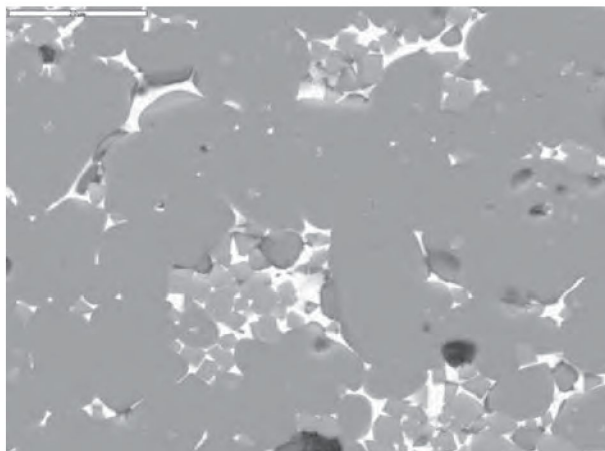


**Fig. 3.** Varistor with unmodified Bi<sub>2</sub>O<sub>3</sub>. Marker 20 μm.

**Rys. 3.** Mikrostruktura warystora domieszkowanego niezmodyfikowanym Bi<sub>2</sub>O<sub>3</sub>.

The amount of Co in the inter-granular layer was about 0.4 mol%. The crystal phases identified in the varistor with Co<sub>2</sub>O<sub>3</sub>-modified Bi<sub>2</sub>O<sub>3</sub> were  $\gamma$ -Bi<sub>2</sub>O<sub>3</sub> (PDF27-53) and the sillenite-type bismuth-cobalt compound (PDF39-871).

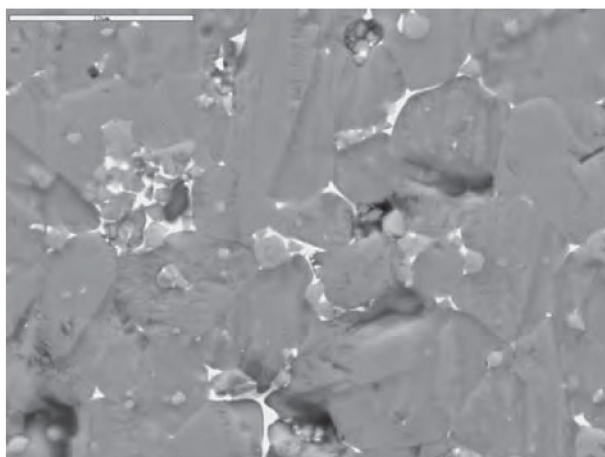


**Fig. 4.** Varistor with Co<sub>2</sub>O<sub>3</sub>-modified Bi<sub>2</sub>O<sub>3</sub>. Marker 20 μm.

**Rys. 4.** Warystora domieszkowany Bi<sub>2</sub>O<sub>3</sub> modyfikowanym Co<sub>2</sub>O<sub>3</sub>.

The intergranular phase in varistor with Mn-modified Bi<sub>2</sub>O<sub>3</sub> is in form of clusters. The ZnO grains (10 μm on average), and the clusters of the Bi<sub>2</sub>O<sub>3</sub>-rich phase

are of similar size (10  $\mu\text{m}$  on average). The clusters of intergranular phase are full of spinel grains (Fig. 5).

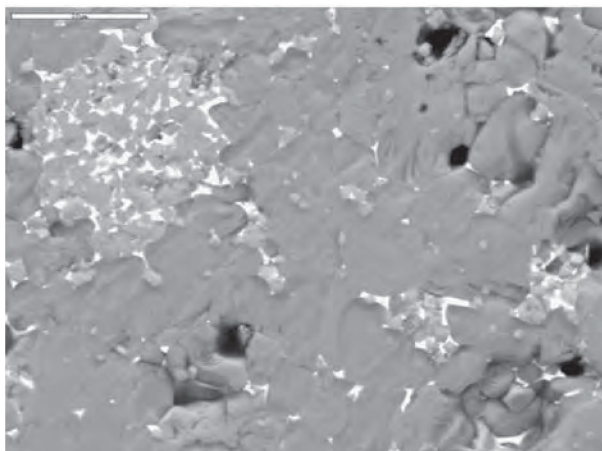


**Fig. 5.** Varistor with MnO-modified Bi<sub>2</sub>O<sub>3</sub>. Marker 20  $\mu\text{m}$ .

**Rys. 5.** Warystor domieszkowany Bi<sub>2</sub>O<sub>3</sub> modyfikowanym MnO.

The crystal phases identified in the varistor with MnO- modified Bi<sub>2</sub>O<sub>3</sub> were zinc-antimony spinel (PDF15-687) and a bismuth oxide crystal phase with the chemical formula Bi<sub>48</sub>ZnO<sub>73</sub> (PDF26-230).

In the varistor with PbO-modified Bi<sub>2</sub>O<sub>3</sub> the ZnO grains were 20- $\mu\text{m}$  large and the agglomerates of the intergranular phase that was completely filled with spinel grains were even larger (Fig. 6).

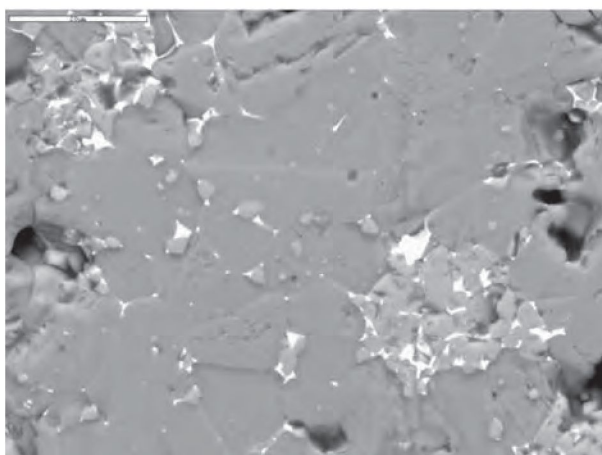


**Fig. 6.** Varistor with PbO-modified Bi<sub>2</sub>O<sub>3</sub>. Marker 20  $\mu\text{m}$ .

**Rys. 6.** Warystor domieszkowany Bi<sub>2</sub>O<sub>3</sub> modyfikowanym PbO.

Pb and Sb were the main elements identified in the inter-granular layer of the varistor with PbO - modified  $\text{Bi}_2\text{O}_3$ . As it comes to crystal phases they were  $\beta\text{-Bi}_2\text{O}_3$  (PDF27-50) and zinc-antimony spinel (PDF15-687)

The varistor with  $\text{Al}_2\text{O}_3$  - modified  $\text{Bi}_2\text{O}_3$  (Fig. 7) was characterized by spherical  $\sim 7 \mu\text{m}$  - large ZnO grains, separated by a glazy inter-granular phase, which also formed  $\sim 10 \mu\text{m}$  - large clusters. The inter-granular phase consisted of Bi and Al atoms, zinc-antimony spinel and  $\text{A}_{12}\text{Bi}_{24}\text{O}_{39}$  (PDF23-1005) phase.

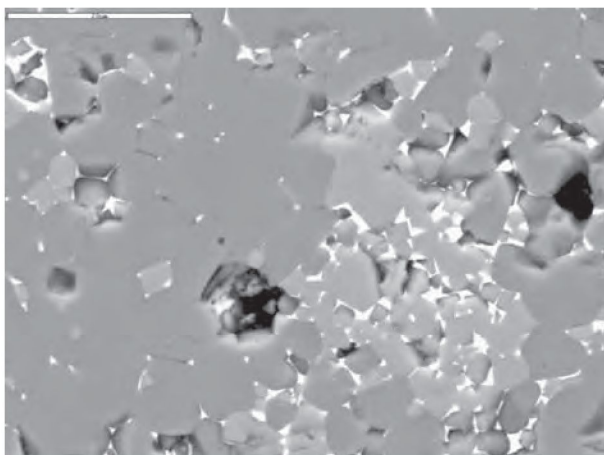


**Fig. 7.** Varistor with  $\text{Al}_2\text{O}_3$  - modified  $\text{Bi}_2\text{O}_3$ . Marker  $20 \mu\text{m}$ .

**Rys. 7.** Warystor domieszkowany  $\text{Bi}_2\text{O}_3$  modyfikowanym  $\text{Al}_2\text{O}_3$ .

The structure of the varistor with  $\text{SiO}_2$ -modified  $\text{Bi}_2\text{O}_3$  was very much similar to that with  $\text{Al}_2\text{O}_3$  modifier. The same spherical  $\sim 7 \mu\text{m}$  - large ZnO grains separated by a glazy inter-granular phase were observed, although the clusters of glazy phase with spinel grains inside it were even larger (Fig. 8). The other crystal phases identified in the varistor with  $\text{SiO}_2$ -modified  $\text{Bi}_2\text{O}_3$  were  $\delta\text{-Bi}_2\text{O}_3$  (PDF27-52) and zinc-antimony spinel (PDF15-687). The Si present in the  $\text{Bi}_2\text{O}_3$  crystal lattice caused the shift of the XRD peaks towards higher angles.

The ZnO grain sizes in the varistor with  $\text{Sb}_2\text{O}_3$ -modified  $\text{Bi}_2\text{O}_3$  were in range of  $10 \mu\text{m}$  (Fig. 9). The inter-granular layer did not form clusters, as in the previously presented samples, but was homogeneously distributed along the ZnO grains. Also, the secondary crystal phases,  $\delta\text{-Bi}_2\text{O}_3$  (PDF27-52) and zinc-antimony spinel (PDF15-687), which are electrically useless elements of the varistor structure, this time occurred in less quantity.



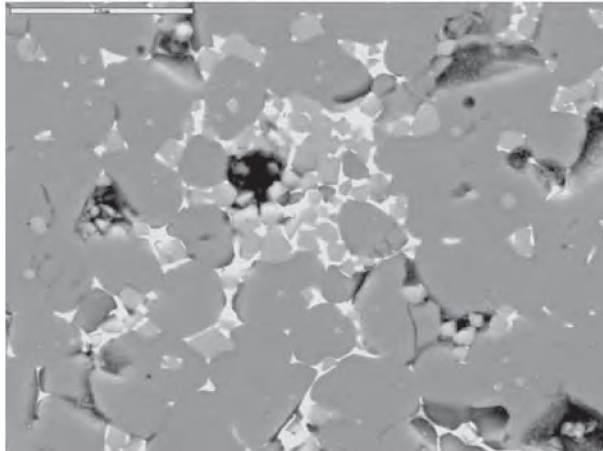


**Fig. 8.** Varistor with  $\text{SiO}_2$  - modified  $\text{Bi}_2\text{O}_3$ . Marker 20  $\mu\text{m}$ .

**Rys. 8.** Warystor domieszkowany  $\text{Bi}_2\text{O}_3$  modyfikowanym  $\text{SiO}_2$ .

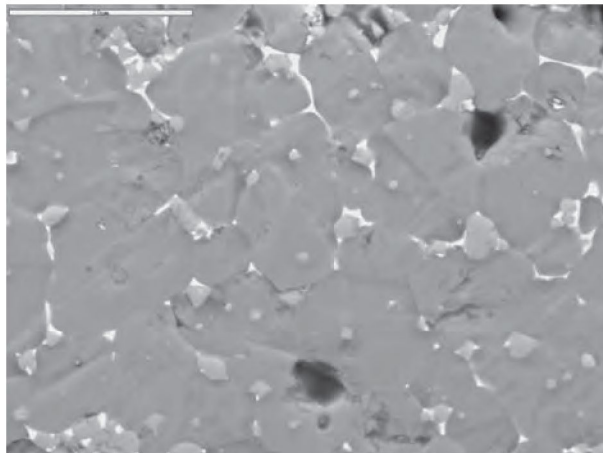


**Fig. 9.** Varistor with  $\text{Sb}_2\text{O}_3$  - modified  $\text{Bi}_2\text{O}_3$ . Marker 20  $\mu\text{m}$ .

**Rys. 9.** Warystor domieszkowany  $\text{Bi}_2\text{O}_3$  modyfikowanym  $\text{Sb}_2\text{O}_3$ .

In the varistor with Sn-modified  $\text{Bi}_2\text{O}_3$  the ZnO grains were 10  $\mu\text{m}$  large. Spinel grains were situated at the junctions of the ZnO grains (Fig. 10), which is beneficial from the point of view of the varistor's electrical properties. When it comes to the inter-granular phase it was, as in case of the Sb modifier, shaped in micron large drops, homogenously distributed along the ZnO grain boundaries. In this varistor all the elements of the varistor structure were homogenously distributed.

The inter-granular phase consisted of Bi and Zn. Sn incorporated into the crystal lattice of spinel. The basic crystal phases were  $\delta$  -  $\text{Bi}_2\text{O}_3$  (PDF27-52) and zinc-antimony spinel (PDF15-687).

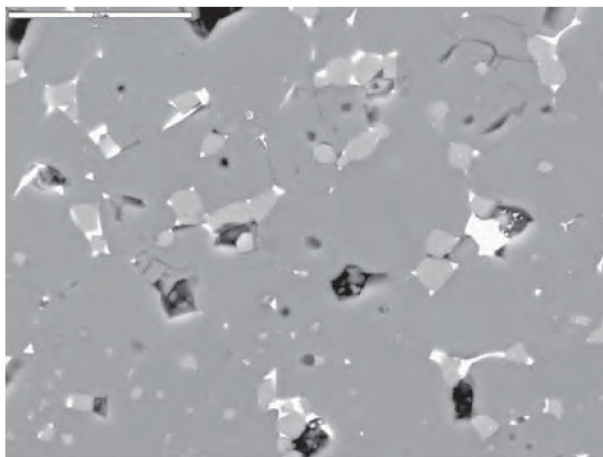


**Fig. 10.** Varistor with  $\text{SnO}_2$ -modified  $\text{Bi}_2\text{O}_3$ . Marker 20  $\mu\text{m}$ .

**Rys. 10.** Warystor domieszkowany  $\text{Bi}_2\text{O}_3$  modyfikowanym  $\text{SnO}_2$ .

The I-V characteristics of varistors doped with modified  $\text{Bi}_2\text{O}_3$  are presented in Fig. 11.

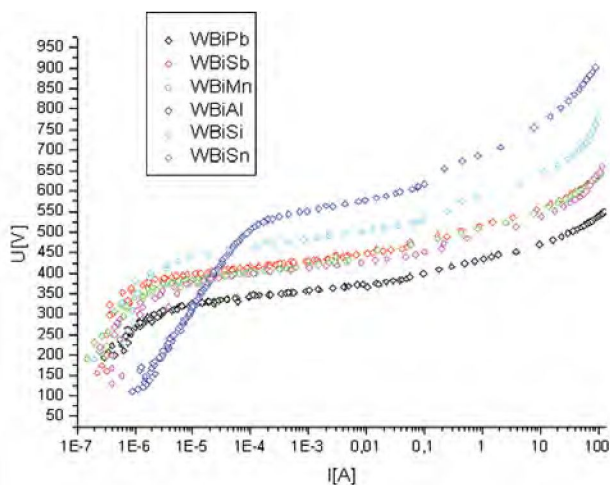


**Fig. 11.** The I-V characteristics of varistors doped with modified  $\text{Bi}_2\text{O}_3$ .

**Rys. 11.** Charakterystyki napięciowo-prądowe warystorów domieszkowanych modyfikowanym  $\text{Bi}_2\text{O}_3$ .

Nonlinearity exponents  $\alpha$ , and characteristic voltages  $V_{0.01-10mA}$  of varistors doped with modified  $\text{Bi}_2\text{O}_3$  are shown in Tab. 3.

**Table 3.** Electrical properties of varistors doped with modified  $\text{Bi}_2\text{O}_3$ .

**Tabela 3.** Własności elektryczne warystorów domieszkowanych modyfikowanym  $\text{Bi}_2\text{O}_3$ .

Sample	$V_{0.01}$ mA [V]	$\alpha$	$V_{0.1}$ mA [V]	$\alpha$	$V_{1 \text{ mA}}$ [V]	$\alpha$	$V_{1/1}$ mA [V]	$\alpha$
Bi085Al	298	5	488	24	539	41	570	263
Bi085Si	403	49	423	55	441	54	460	223
Bi085Sn	451	48	474	60	492	82	506	242
Bi085Sb	432	47	454	58	473	55	493	236
Bi085Mn	390	45	411	55	428	44	452	210
Bi085Pb	315	33	352	45	371	45	391	199

The highest non-linear coefficients ( $\alpha = 55-58$ ), were obtained for varistors doped with Sb modified  $\text{Bi}_2\text{O}_3$ . Along with it the varistor gradient  $V_{1/1}$  slightly (to 236 V/mm) decreased, what is desired. The further decrease of  $V_{1/1}$  was attained with Pb, Sn and Mn modifiers while Al caused the  $V_{1/1}$  increase and  $\alpha$  coefficients decrease.

#### 4. CONCLUSIONS

The microstructure of the typical varistor is characterized by some non-uniformity. The preliminary  $\text{Bi}_2\text{O}_3$  modification, even with small amounts of other metal oxides, causes significant changes to the varistor's structure. No such effect is observed when the MeO modifiers and the  $\text{Bi}_2\text{O}_3$  are added directly to the varistor mixture, without a preliminary reaction between themselves.

Glazy-forming Me modifiers, like  $\text{SiO}_2$ ,  $\text{Al}_2\text{O}_3$ , PbO or MnO, do not help much when it comes to homogenization of varistor structure, and they also do not prevent the formation of harmful and electrically useless regions in varistor.

However, the varistor derives substantial benefit from  $\text{Bi}_2\text{O}_3$  modification with  $\text{Sb}_2\text{O}_3$  and  $\text{SnO}_2$ . In the case of the  $\text{Sb}_2\text{O}_3$  modifier an inter-granular phase is homogeneously distributed along the ZnO grains, moreover, crystal phases occurs in less amount. With  $\text{SnO}_2$  modifier, varistor structure benefits even more.

As  $\text{Sb}_2\text{O}_3$  and  $\text{SnO}_2$  facilitate the homogeneous distribution of additives in varistor body they would enable the decrease of the amount of additives and elimination

W. Mielcarek, K. Prociów, J. Warycha

of an electrically inactive areas from varistor body what would bring about the diminishment of the cost of varistors processing along with improvement of their performance.

## ACKNOWLEDGMENT

*The authors gratefully acknowledge the support of the Ministry of Science and Higher Education under grant No N N 510 344 534*

## REFERENCES

- [1] Kosman M. S., Gesse J.A.: Dielektričeskaja pronikajemost okisi cinka s primiestju okisi bismuta, *Izvest. Akad. Nauk SSR Ser. Fiz.*, 22, 3, (1958), 315
- [2] Matsuoka M., Masuyamai T., Iida Y.: Voltage nonlinearity of zinc oxide ceramics doped with alkali earth metal oxide, *Jpn. J. Appl. Phys.*, (1969 ), 1275
- [3] Hohenberger G., Tomandl G., Ebert R., Taube V.: Inhomogeneous conductivity in varistor ceramics methods of investigation, *J. Am. Ceram. Soc.*, 74, 9, (1991), 2067

## MOŻLIWOŚCI MODYFIKACJI MIKROSTRUKTURY WARYSTORÓW TLENKOWYCH

Własności elektryczne warystorów, podobnie jak pozystorów i innych wyrobów z ceramiki półprzewodnikowej, są kontrolowane przez ukształtowanie granicy ziaren. Ceramika warystorowa ZnO swoje niewłaściwości elektryczne zawdzięcza domieszce małej ilości innych tlenków metali. Mikrostruktura warystora rozwija się podczas spiekania. Głównym elementem mikrostruktury warystora są ziarna ZnO odseparowane od siebie cienką, bogatą w bizmut, warstwą międzyziarnową. Najlepsze własności elektryczne warystor wykazuje wtedy, kiedy warstwa ta jest możliwie cienka. Jeżeli warstwa ta jest w formie aglomeratów, a w dodatku zawiera w sobie wykryształizowany  $\text{Bi}_2\text{O}_3$  lub krystality innych związków to tworzy obszar wykluczony z przewodnictwa. W warystorze o takiej strukturze w czasie przepływu prądu dochodzi do miejscowych przegrzań i zakłóceń w działaniu. W pracy udowodniono doświadczalnie, że spiekając wstępnie tlenek bizmutu z tlenkami innych metali można wpływać na kształt warstwy międzyziarnowej, a więc i na elektryczne własności warystora. Przeprowadzone doświadczenia dowiodły, że jeżeli  $\text{Bi}_2\text{O}_3$  przed dodaniem do warystora spieczemy wstępnie z tlenkami Co, Sb lub Sn to tak zmodyfikowany tlenek bizmutu sprzyja równomiernemu rozproszczeniu domieszek



w warystorze przyczyniając się do eliminacji ze struktury warystora obszarów nieaktywnych elektrycznie. Natomiast wstępne modyfikowanie tlenku bizmutu tlenkami tzw. szkłotwórczymi jak PbO, SrO i MnO nie przynosi podobnego efektu.

**Słowa kluczowe:** warystor ZnO, mikrostruktura, ceramika półprzewodnikowa, domieszkowanie,  $\text{Bi}_2\text{O}_3$